Structure-Dependent Photophysics of First-Generation Phenyl-Cored Thiophene Dendrimers

William J. Mitchell, Andrew J. Ferguson,* Muhammet E. Köse, Benjamin L. Rupert, David S. Ginley, Garry Rumbles, Sean E. Shaheen, and Nikos Kopidakis

National Renewable Energy Laboratory, 1617 Cole Boulevard, Golden, Colorado, 80401−3393

Received September 5, 2008. Revised Manuscript Received October 21, 2008

We have prepared two series of first-generation thiophene-bridge dendrimers, with either three (3G1) or four (4G1) arms attached to a phenyl core, to elucidate their structure−property relationships. Optical properties were investigated with a combination of steady-state and time-resolved spectroscopic techniques. Steady-state spectroscopic data for the 3-arm dendrimers suggests that the exciton is delocalized over the α-conjugated thiophene segment and the phenyl core, but that the meta-linking of the dendrons prevents their electronic communication. In contrast, conjugation through the core to dendrons in the ortho and para positions is permitted in the 4-arm dendrimers, although the data suggest that the conjugation length does not extend over the full length of the α-conjugated sections of two coupled dendrons. This observation is due to steric interactions between neighboring arms, which forces the arms to twist and bend out of the plane of the phenyl core, and is particularly prevalent in disrupting the conjugation through the ortho positions. As expected, our results show that an increase in the bridge length results in an increase in the conjugation length for both dendrimers, and a subsequent red-shift of the absorption and emission. In addition, an increase in the dendron length results in an increase in the photoluminescence quantum yield and lifetime, suggesting that the ground and excited-state geometries are very similar and that the electronic transition is coupled to fewer vibrational modes.

Introduction

Conjugated dendrimers provide an excellent material set to supplement conjugated polymers in the arena of organic electronics.[1] They offer the processability of polymers for device applications, but they also provide precisely defined molecular structures that allow for systematic study of structure−property relationships such as the theoretical description of their structure-dependent optical and electronic properties.[2−4] It is through studies of conjugated dendrimers that clear and distinct structure−property relationships can be elucidated that may ultimately lead to improvement in performance of devices such as organic light-emitting diodes (OLEDs),[1,5] organic photovoltaic (OPV),[1,6−9] and other optoelectronic devices.

Dendrimers are macromolecules with a precisely defined structure consisting of dendrons attached to a central core. The dendrons are typically branched, and the degree of the branching is known as the "generation" of the dendrimer. Depending on the desired function the dendrons can be aliphatic or the structure as a whole can be conjugated.[10,11] Conjugated dendrimers possess several possible advantages over their analogous polymers for use in optoelectronic applications, including a well-defined molecular weight, improved batch-to-batch reproducibility and a higher degree of purity. Such dendrimers have previously been synthesized with dendrons containing phenylacetylene,[12,13] phenylene,[14] and phenylenevinylene[15−17] units, and more recently dendrimers have been prepared that are conjugated through thiophene repeat units.[18−21] Thiophene has been extensively utilized as the foundation of many optoelectronic organic materials[18−24] including polymers, oligomers, and more

* Corresponding author. E-mail: andrew_ferguson@nrel.gov.

(1) Lo, S. C.; Burn, P. L. *Chem. Rev.* **2007**, *107*, 1097.
(2) Lupton, J. M.; Samuel, I. D. W.; Beavington, R.; Frampton, M. J.; Burn, P. L.; Bassler, H. *Phys. Rev. B* **2001**, *63*, 155206.
(3) Supritz, C.; Engelmann, A.; Reineker, P. *J. Lumin.* **2006**, *119*, 337.
(4) Köse, M. E.; Mitchell, W. J.; Kopidakis, N.; Chang, C. H.; Shaheen, S. E.; Kim, K.; Rumbles, G. *J. Am. Chem. Soc.* **2007**, *129*, 14257.
(5) Markham, J. P. J.; Lo, S. C.; Magennis, S. W.; Burn, P. L.; Samuel, I. D. W. *Appl. Phys. Lett.* **2002**, *80*, 2645.
(6) Brabec, C. J.; Sariciftci, N. S.; Hummelen, J. C. *Adv. Funct. Mater.* **2001**, *11*, 15.
(7) Coakley, K. M.; McGehee, M. D. *Chem. Mater.* **2004**, *16*, 4533.
(8) Shaheen, S. E.; Ginley, D. S.; Jabbour, G. E. *MRS Bull.* **2005**, *30*, 10.
(9) Kopidakis, N.; Mitchell, W. J.; van de Lagemaat, J.; Ginley, D. S.; Rumbles, G.; Shaheen, S. E.; Rance, W. L. *Appl. Phys. Lett.* **2006**, *89*, 103524.
(10) Matthews, O. A.; Shipway, A. N.; Stoddart, J. F. *Prog. Polym. Sci.* **1998**, *23*, 1.
(11) Adronov, A.; Frechet, J. M. J. *Chem. Commun.* **2000**, 1701.
(12) Hu, Q. S.; Pugh, V.; Sabat, M.; Pu, L. *J. Org. Chem.* **1999**, *64*, 7528.
(13) Peng, Z. H.; Pan, Y. C.; Xu, B. B.; Zhang, J. H. *J. Am. Chem. Soc.* **2000**, *122*, 6619.
(14) Berresheim, A. J.; Muller, M.; Mullen, K. *Chem. Rev.* **1999**, *99*, 1747.
(15) Pillow, J. N. G.; Halim, M.; Lupton, J. M.; Burn, P. L.; Samuel, I. D. W. *Macromolecules* **1999**, *32*, 5985.
(16) Beavington, R.; Frampton, M. J.; Lupton, J. M.; Burn, P. L.; Samuel, I. D. W. *Adv. Funct. Mater.* **2003**, *13*, 211.
(17) Diez-Barra, E.; Garcia-Martinez, J. C.; del Rey, R.; Rodriguez-Lopez, J.; Giacalone, F.; Segura, J. L.; Martin, N. *J. Org. Chem.* **2003**, *68*, 3178.
(18) Xia, C. J.; Fan, X. W.; Locklin, J.; Advincula, R. C.; Gies, A.; Nonidez, W. *J. Am. Chem. Soc.* **2004**, *126*, 8735.
(19) Ponomarenko, S. A.; Kirchmeyer, S.; Elschner, A.; Huisman, B. H.; Karbach, A.; Drechsler, D. *Adv. Funct. Mater.* **2003**, *13*, 591.
(20) Mitchell, W. J.; Kopidakis, N.; Rumbles, G.; Ginley, D. S.; Shaheen, S. E. *J. Mater. Chem.* **2005**, *15*, 4518.
(21) Ma, C. Q.; Mena-Osteritz, E.; Debaerdemaeker, T.; Wienk, M. M.; Janssen, R. A. J.; Bauerle, P. *Angew. Chem., Int. Ed.* **2007**, *46*, 1679.
(22) McCullough, R. D. *Adv. Mater.* **1998**, *10*, 93.

10.1021/cm802410d CCC: $40.75
Published on Web 12/24/2008

recently dendrimers, which have been used in OLEDs,[25−30] field-effect transistors (FETs),[19,31−34] and in OPV devices.[35,36] The structure of a given dendrimer can be fine-tuned to attain the desired properties by introducing a variety of substituents either into the backbone or as sidegroups.[1,37−40]

We recently reported on a new class of thiophene dendrimers in which fully conjugated thiophene dendrons were attached to a phenyl core,[20] and subsequently used the dendrimers as a light-absorber in the active layer of bulk heterojunction OPV devices, which demonstrated that reducing the band gap by increasing the length of the dendron lead to increased efficiency.[9] The dendrimers prepared had either three or four dendrons, with either one or two branching points, around the core: the molecular structures of the first generation dendrimers are shown in Figure 1. The nomenclature *x*G*y*-*n*S describes the dendrimers where *x* is the number of dendrons of *y* generation ($y = 1$ in this study), and *n* is the number of bridging thiophene moieties.

Here we report the convergent synthesis of four new first-generation conjugated thiophene dendrimers that form part of a long-term study to examine correlations among theoretical description,[4] molecular structure and properties,[20] and device performance.[9] We introduce extended thiophene bridges between the branching point and the core to give structures with *n* equal to either two or three, and compare the photophysical properties of these four dendrimers to 3G1−1S and 4G1−1S ($n = 1$ in Figure 1) from our previous study.[20]

We show that the chromophore in the 3-arm dendrimer is delocalized over the α-conjugated thiophene segment and the phenyl core, but that the meta-linking of the dendrons prevents delocalization of the exciton over the entire structure, consistent with the observed optical properties of oligophenylenevinylene dendrimers.[16,41] In contrast, ortho- and para-substitution in the 4-arm dendrimers permits electronic communication between two dendrons, although the effective conjugation length is smaller than the length of two α-conjugated segments coupled through the phenyl core because of steric interactions between neighboring arms. Extending the length of the dendron bridging group is shown to systematically lower the optical band gap of the material, but also results in an increase in the photoluminescence quantum yield and lifetime, suggesting more similar geometries for the ground and excited states, as well as a reduction in electron−phonon coupling. Additionally, the increase in thiophene bridge length is thought to relieve the steric interaction between the peripheries of the dendrons for the 4G1 series, resulting in a more planar structure. The experimentally observed optical properties are consistent with predictions made previously in a theoretical study using ab initio methods.[4]

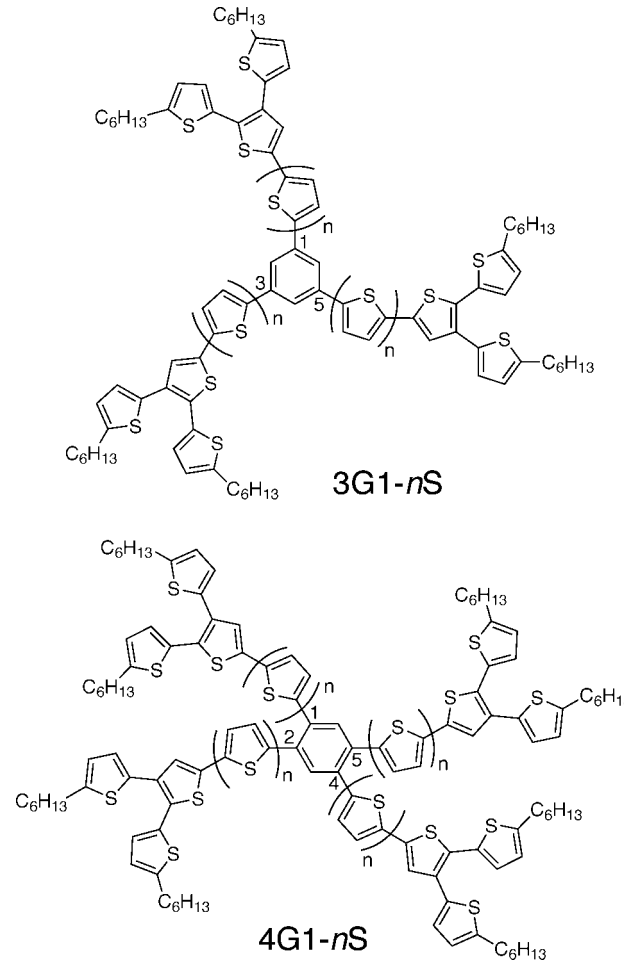

Figure 1. General structures of the 1st generation phenyl-cored thiophene-bridge dendrimers: *n* denotes the number of bridging thiophene rings between the phenyl core and branching point of the dendron. The substitution positions of the dendrons around the phenyl core are numbered consistent with the descriptions used throughout the text.

Synthesis

The synthetic route to the first generation dendrons is shown in Scheme 1 and that of the dendrimers in Scheme 2. The dendrimers were prepared by the convergent synthesis method where the core and dendrons are prepared separately and then united in the final step to form the dendrimer.

(23) Fichou. D. *Handbook of Oligo- and Polythiophenes*; Wiley-VCH: New York, 1998.
(24) Xia, C. J.; Fan, X. W.; Locklin, J.; Advincula, R. C. *Org. Lett.* **2002**, *4*, 2067.
(25) Braun, D.; Gustafsson, G.; McBranch, D.; Heeger, A. J. *J. Appl. Phys.* **1992**, *72*, 564.
(26) Geiger, F.; Stoldt, M.; Schweizer, H.; Bauerle, P.; Umbach, E. *Adv. Mater.* **1993**, *5*, 922.
(27) Granstrom, M. *Polym. Advan. Technol.* **1997**, *8*, 424.
(28) Gigli, G.; Anni, M.; Theander, M.; Cingolani, R.; Barbarella, G.; Favaretto, L.; Inganas, O. *Synth. Met.* **2001**, *119*, 581.
(29) Mazzeo, M.; Pisignano, D.; Favaretto, L.; Barbarella, G.; Cingolani, R.; Gigli, G. *Synth. Met.* **2003**, *139*, 671.
(30) Markham, J. P. J.; Namdas, E. B.; Anthopoulos, T. D.; Samuel, I. D. W.; Richards, G. J.; Burn, P. L. *Appl. Phys. Lett.* **2004**, *85*, 1463.
(31) Dodabalapur, A.; Torsi, L.; Katz, H. E. *Science* **1995**, *268*, 270.
(32) Lovinger, A. J.; Rothberg, L. J. *J. Mater. Res.* **1996**, *11*, 1581.
(33) Sirringhaus, H.; Brown, P. J.; Friend, R. H.; Nielsen, M. M.; Bechgaard, K.; Langeveld-Voss, B. M. W.; Spiering, A. J. H.; Janssen, R. A. J.; Meijer, E. W.; Herwig, P.; de Leeuw, D. M. *Nature* **1999**, *401*, 685.
(34) McCulloch, I.; Heeney, M.; Bailey, C.; Genevicius, K.; Macdonald, I.; Shkunov, M.; Sparrowe, D.; Tierney, S.; Wagner, R.; Zhang, W. M.; Chabinyc, M. L.; Kline, R. J.; McGehee, M. D.; Toney, M. F. *Nat. Mater.* **2006**, *5*, 328.
(35) Padinger, F.; Rittberger, R. S.; Sariciftci, N. S. *Adv. Funct. Mater.* **2003**, *13*, 85.
(36) Li, G.; Shrotriya, V.; Huang, J. S.; Yao, Y.; Moriarty, T.; Emery, K.; Yang, Y. *Nat. Mater.* **2005**, *4*, 864.
(37) Roncali, J. *Chem. Rev.* **1997**, *97*, 173.
(38) Greiner, A. *Polym. Adv. Technol.* **1998**, *9*, 371.
(39) Huang, W.; Meng, H.; Yu, W. L.; Gao, J.; Heeger, A. J. *Adv. Mater.* **1998**, *10*, 593.
(40) Mitschke, U.; Bauerle, P. *J. Mater. Chem.* **2000**, *10*, 1471.

Scheme 1. Synthesis of G1−2S Dendron (4) and the Corresponding Stannane (5)

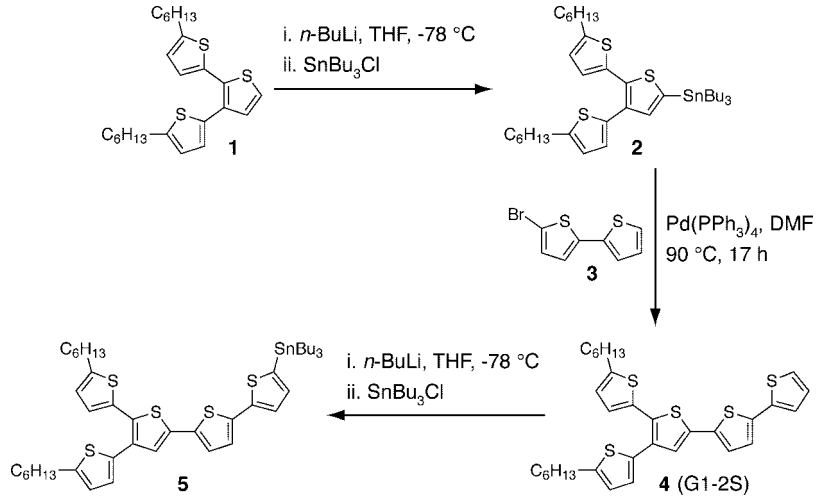

The first-generation dendron **1** was prepared by literature procedures.[24] Alkylation of thiophene by sequential deprotonation with butyllithium and addition of 1-bromohexane followed by bromination gave 1-bromo-5-hexylthiophene in an overall 86% yield. The corresponding Grignard reagent was prepared and reacted with 2,3-dibromothiophene in a nickel-catalyzed Kumada coupling to give the G1 dendron **1** in 52% yield. Extension of dendron **1** to give extended dendron **4** was then accomplished by Stille reaction with 2-bromo-bithiophene **3**:[42] the stannane of dendron **1** was synthesized by lithiation with butyllithium at −78 °C followed by quenching of the formed lithium salt with tributyltin chloride. The stannane functionalized dendron **2** was used without purification and undertook Stille coupling with bithiophene **3** to give G1−2S **4** in 81% yield, after isolation by column chromatography.

The four first-generation dendrimers (**7**, **9**, **11**, **13**) were prepared following the synthetic route outlined in Scheme 2. All four dendrimers were prepared via Stille coupling of the relevant core and the stannane **5** of the G1−2S dendron **4**. The stannane **5** was synthesized by initial reaction with butyllithium at −78 °C before warming to room temperature and further reaction with tributyltin chloride to give the desired stannane, which was used without purification. The core **6**,**8**,[20] **10**, or **12**[20] and G1−2S stannane dendron **5** in dry *N*,*N*-dimethylformamide was initially degassed with argon followed by addition of the palladium catalyst and the mixture heated at 90 °C for 50 h. Work-up and purification by repeated washings with acetone until the filtrate was colorless gave dendrimers **7** (3G1−2S), **9** (3G1−3S), **11** (4G1−2S), and **13** (4G1−3S) in excellent yields for the two steps from dendron **4** of 85, 88, 94, and 86%, respectively.

The four dendrimers were solid and ranged in color from orange to red. All the dendrimers were soluble in common organic solvents such as chloroform, THF, and toluene, but polar solvents such as methanol and DMSO were very poor solvents. However, the solubilities of the 3G1 dendrimers were lower, probably because of greater planarity and the lower number of solubilizing alkyl groups on the dendrons. The solubility of the 3G1−3S was much reduced, and only low concentrations of dendrimer were attainable.

The structures and purity of the dendrimers were confirmed by ^{1}H and ^{13}C nuclear magnetic resonance (NMR) spectroscopy, matrix-assisted laser desorption/ionization time-of-flight (MALDI-TOF) mass spectrometry and microanalysis, whereas the thermal decomposition was monitored using thermogravimetric analysis (TGA). The solution-phase electronic properties of the dendrimers were investigated using cyclic voltammetry (CV); see the Supporting Information for a more detailed discussion of the MALDI-TOF (Figure S2), TGA (Figure S3), and CV (Figures S4 and S5) data.

Photophysical Properties. The optical absorption spectra of the four dendrimers [3G1−2S (**7**), 3G1−3S (**9**), 4G1−2S (**11**), and 4G1−3S (**13**)] in dichloromethane (DCM) are shown in Figure 2. The spectra for the G1−2S dendron, and the 3G1−1S and 4G1−1S dendrimers, have been included for comparison. The corresponding optical absorption properties are summarized in Table 1.

The normalized photoluminescence spectra, corrected for the spectral response of the detection system, of the six dendrimers [3G1−1S, 3G1−2S (**7**), 3G1−3S (**9**), 4G1−1S, 4G1−2S (**11**), and 4G1−3S (**13**)] upon excitation at 445 nm are presented in Figure 3, along with the results from the spectral fitting routine (see the Experimental Section for more details). Photoluminescence decays, after excitation at 438 nm, are shown for the same dendrimers in Figure 4. Finally, the corresponding photoluminescence properties are summarized in Table 2.

The dependence of the optical properties, particularly the energy of the optical band gap (estimated from either the absorption onset or the electronic origin of the emission, which is defined as the energy of the transition between the lowest vibrational levels of the excited state and ground state), on the number of dendrons around the core and the number of bridging thiophene rings between the core and branching point of the dendron are discussed in further detail in the following section.

(41) Lupton, J. M.; Samuel, I. D. W.; Burn, P. L.; Mukamel, S. *J. Phys. Chem. B* **2002**, *106*, 7647.
(42) Wu, R. L.; Schumm, J. S.; Pearson, D. L.; Tour, J. M. *J. Org. Chem.* **1996**, *61*, 6906.

Scheme 2. Synthesis of First-Generation Phenyl-Cored Thiophene-Bridge Dendrimers (7, 9, 11, and 13)

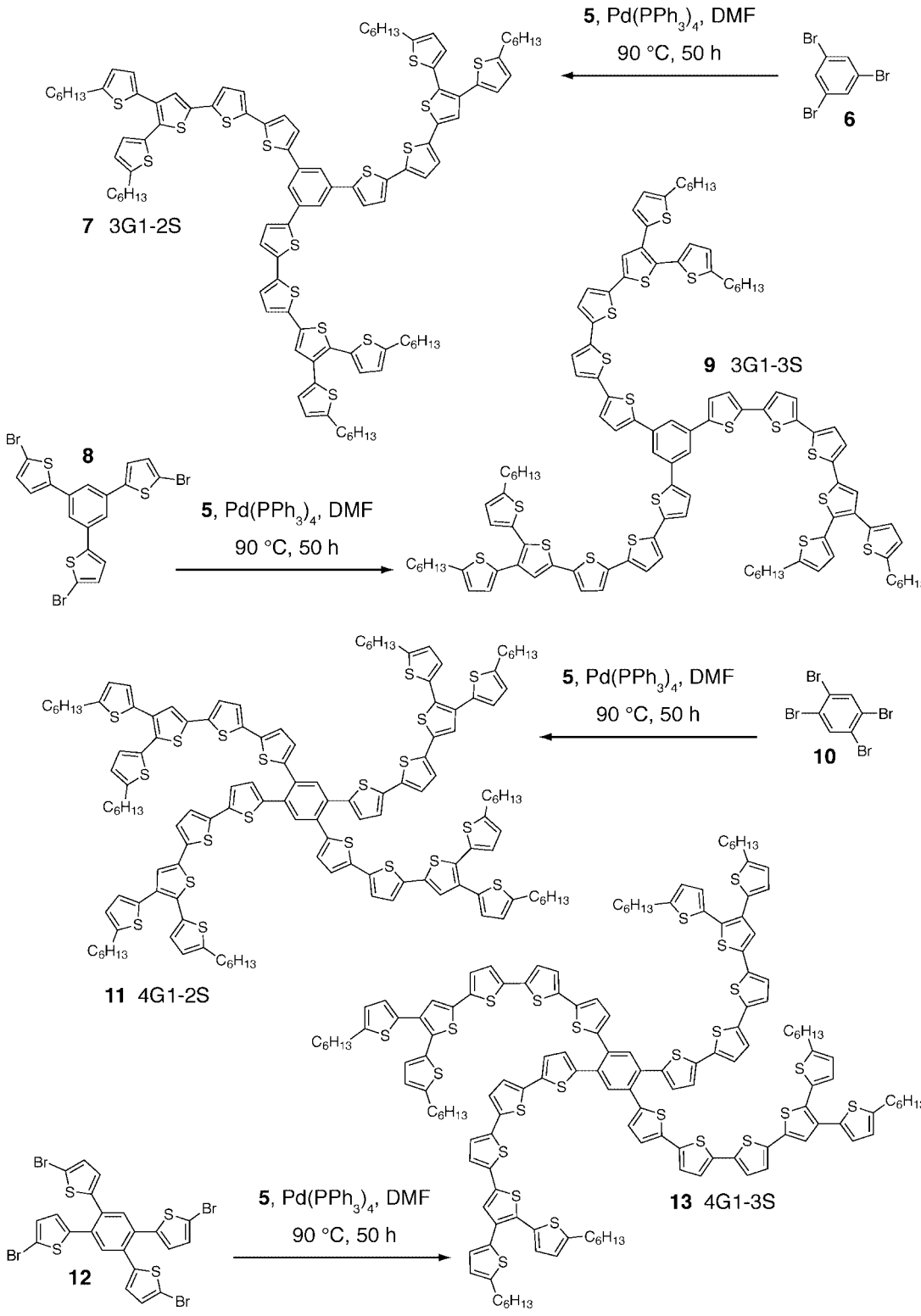

Discussion

The linkages between adjacent thiophenes within the dendrons are either considered α−α or α−β connections, with the former giving the greater π-conjugation. All the dendrimers possess one α−β connection at the periphery of each dendron, but the remaining linkages are all α−α connections; consequently, the conjugation length of the dendron is directly correlated to the number of bridging thiophene units, n. The maximum possible α-conjugation length of the dendron is given by $n + 2$. Therefore, the longest thiophene conjugation sequences are an α-terthiophene, α-quarterthiophene or α-pentathiophene, for the 1S, 2S, and 3S dendrimers respectively.

The absorption onset of 3G1−1S lies at 2.70 eV (460 nm), very close to the value for the α-quarterthiophene-based oligomers and dendrimers,[19,21,43] including the G1−2S dendron, implying that the main chromophore consists of a four-ring system. Because the longest thiophene chain is an

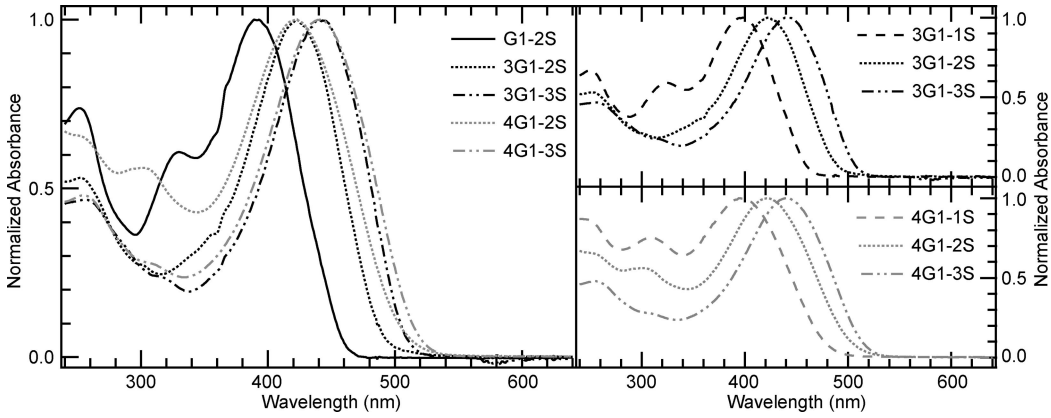

Figure 2. Optical absorption spectra of the first-generation phenyl-cored thiophene-bridge dendrimers in dichloromethane: the left panel shows a comparison between the 3- and 4-arm dendrimers (the absorption spectrum of the G1−2S dendron is shown for comparison), whereas the right-hand panels show the effect of increased dendron length on the 3-arm (upper) and 4-arm (lower) dendrimers.

Table 1. Optical Absorption Properties of First-Generation Phenyl-Cored Thiophene-Bridge Dendrimers in Dichloromethane

comd	E_{ons}^{abs} (eV (nm))[a]	E_{max}^{abs} (eV (nm))[b]	ε_{max} ($M^{-1}cm^{-1}$)
G1−2S	2.71 (457)	3.18 (390)	
3G1−1S[c]	2.70 (460)	3.11 (399)	85 000
3G1−2S (**7**)	2.53 (490)	2.93 (423)	109 000
3G1−3S (**9**)	2.44 (508)	2.82 (440)	130 000
4G1−1S[c]	2.53 (491)	3.13 (396)	115 000
4G1−2S (**11**)	2.39 (518)	2.94 (422)	156 000
4G1−3S (**13**)	2.36 (525)	2.81 (442)	143 000

[a] Energy of the absorption onset; wavelength given in parentheses. [b] Energy of the absorption maximum; wavelength given in parentheses. [c] Optical properties of 3G1−1S and 4G1−1S from previous study.[20]

α-terthiophene this suggests that the dendrons are conjugated to the phenyl core, consistent with recent theoretical calculations.[4] This observation also implies that the extra α−β linked thiophene at the periphery of each dendron has little impact on the conjugation within the all α-linked quarterthiophene unit, contrary to observations for higher generation thiophene dendrons.[21]

Incorporation of four G1−1S dendrons around the phenyl core results in significant broadening of the absorption, and the absorption onset and electronic origin of the emission are red-shifted by 170 and 230 meV, respectively, compared to 3G1−1S. A red-shift is also observed for the absorption onset and electronic origin of the emission for 4G1−2S and 4G1−3S compared to the equivalent 3-arm dendrimer. The magnitude of this shift decreases with increasing thiophene bridge length; 1S (170 meV/230 meV), 2S (140 meV/150 meV), and 3S (80 meV/90 meV), due to decreasing relative extension of the conjugation length of the chromophore. We do not attribute these red-shifted 4G1-*n*S spectra to intermolecular interactions resulting from physical dimer formation; instead, the ortho and para relationship of the dendrons permits delocalization through the phenyl core, resulting in an increase in the conjugation length of the chromophore, consistent with ab initio calculations reported for these dendrimers[4] as well as experimental studies of phenylacetylene dendrimers[44] and oligophenylenevinylenes.[45] However, it should be noted that the red shifts are not as large as would be expected for a conjugation length almost twice as long in the 4G1 series and we attribute this discrepancy to steric hindrance between the arms ortho to each other, which forces the dendrons to twist and bend out of the plane of the phenyl core.[4] Figure 5 shows a plot of the absorption onset energy and the electronic origin of the emission as an inverse function of the effective conjugation length of the chromophore, which is defined by the number of atoms, a, in the conjugated segment.[46] If the addition of a ring to the thiophene bridge results in an identical increase in the length of the chromophore then such a plot should show a linear dependence of energy vs inverse number of atoms.[47] Figure 5 indicates that such behavior is observed for the 3G1 dendrimers, where the solid lines are linear fits through the data, and correspond to the number of atoms in a single α-conjugated segment plus the phenyl core. In contrast, if the chromophore in the 4G1 series is assumed to extend through the core and over the full length of two arms then the crosses in Figure 5 would fall on the solid lines and the expected red-shift of the absorption onset and electronic origin of the emission would be larger than is observed experimentally. This is clearly not the case, suggesting that the chromophore does not extend through the phenyl core and over all α-conjugated thiophene rings in two arms, whether or not they are arranged ortho or para to each other. If one invokes a restriction of the conjugation length, consistent with distortion from planarity because of steric effects in neighboring arms and thermal motion of the thiophene rings at the end of the dendrons, the data is consistent with the observed trend for the 3-arm dendrimers; the open squares lie on the solid lines in Figure 5. It should be noted that this requires that the effective conjugation length be reduced to roughly 5−6 rings for 4G1−1S, 6−7 rings for 4G1−2S, and 7 rings for 4G1−3S.

Recent theoretical calculations for two thiophene dendrons bound in different arrangements around a phenyl core

(43) Pham, C. V.; Burkhardt, A.; Shabana, R.; Cunningham, D. D.; Mark, H. B.; Zimmer, H. *Phosphorus Sulfur* **1989**, *46*, 153.
(44) Melinger, J. S.; Pan, Y. C.; Kleiman, V. D.; Peng, Z. H.; Davis, B. L.; McMorrow, D.; Lu, M. *J. Am. Chem. Soc.* **2002**, *124*, 12002.
(45) Karabunarliev, S.; Baumgarten, M.; Tyutyulkov, N.; Mullen, K. *J. Phys. Chem.* **1994**, *98*, 11892.
(46) Four atoms are counted for each thiophene ring (the sulfur atom is not included) and six atoms corresponding to the phenyl core. For both the 3G1 and 4G1 dendrimers, the beta-linked thiophene rings are not included in calculations of the effective conjugation length.
(47) Hutchison, G. R.; Zhao, Y. J.; Delley, B.; Freeman, A. J.; Ratner, M. A.; Marks, T. J. *Phys. Rev. B* **2003**, 68.

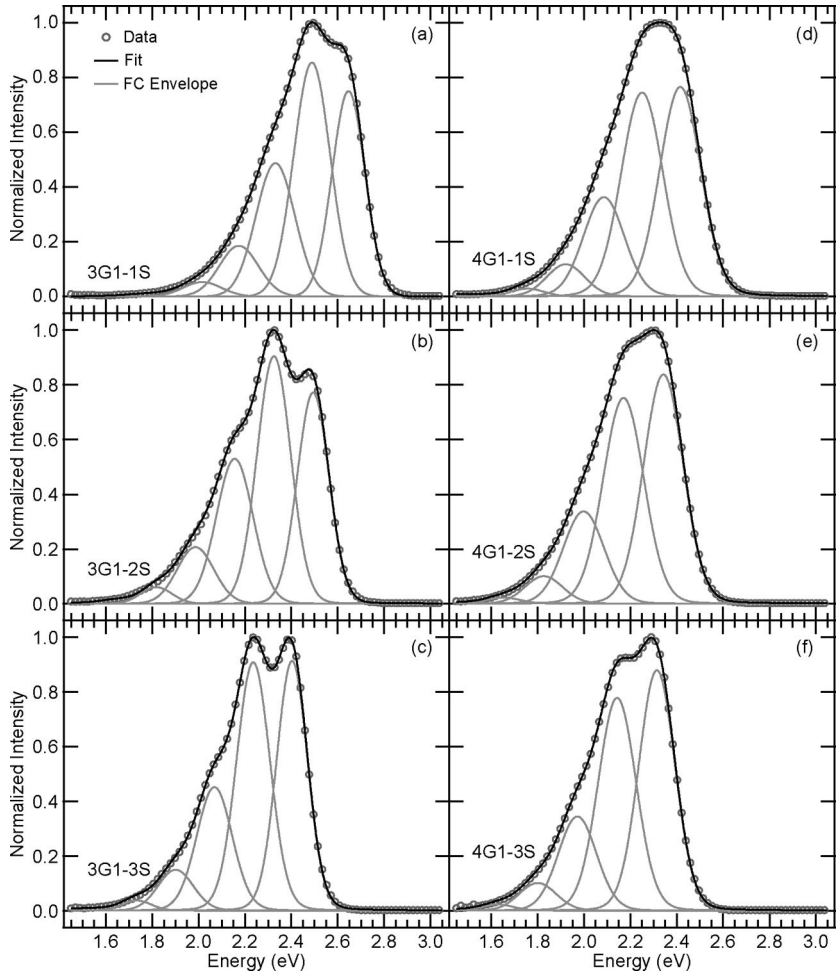

Figure 3. Normalized photoluminescence spectra (○), corrected for the spectral response of the detection system, for (a) 3G1−1S, (b) 3G1−2S, (c) 3G1−3S, (d) 4G1−1S, (e) 4G1−2S, and (f) 4G1−3S in degassed chloroform. Also shown are the fit (solid black lines) and Franck−Condon (FC) envelope (solid gray lines) from the spectral fitting process.

confirm exciton localization over one arm and the core in the meta-linked case, but no electronic coupling between the arms,[4] consistent with the experimental observations for 3G1−1S and independent studies on phenylacetylene dendrimers[44,48] and oligophenylenevinylenes.[16,41,45] Conversely, electronic coupling is permitted between arms in either an ortho or para relationship to each other, with a stronger interaction between para-linked arms.[4] Density functional theory geometry optimization of the ground-state of 4G1−1S indicates a more planar arrangement of the thiophene dendrons in the 1- and 4- positions (dihedral angle ∼40° between the planes of the core and the adjacent thiophene unit), whereas a larger dihedral angle is observed for the arms at the 2- and 5- positions (∼56°); the ends of these dendrons are also bent further out of the plane of the phenyl core.[4] It should be noted that increasing the length of the thiophene bridge has negligible impact on these dihedral angles, suggesting that the steric interaction between thiophene rings bound directly to the core is solely responsible for the extent of twisting relative to the phenyl ring. As a result of the predicted structure, the "hot" exciton, resulting from photon absorption, is localized over all dendrons in 4G1−1S, although enhanced coupling is observed between the arms at the 1- and 4-positions. Significant structural reorganization occurs to yield the "cold" exciton (dihedral angles at the 1-/4- and 2-/5-positions are ∼7 and 75°, respectively), from which radiative relaxation occurs to give emission, resulting in localization of the excitation over the dendrons at the 1- and 4-positions, but with the arms in a more coplanar arrangement with the core.[4] A similar planarization of the arms at the 1- and 4-positions occurs for the 4G1−2S and 4G1−3S dendrimers, albeit with slightly larger dihedral angles (data not shown). In contrast, the arms at the 2- and 5-positions are twisted less out of the plane of the phenyl core in the "cold" exciton of the larger 4-arm dendrimers. These observations indicate a decreasing geometrical rearrangement to form the "cold" exciton as the thiophene bridge length increases, implying that the nature of the emitting exciton changes in the 4G1 series, which goes some way to explaining the variation in the calculated natural radiative lifetime (see discussion below).

As expected, extension of the bridging unit between the core and branching point of the dendron gives rise to a red-shifted absorption and emission spectra; the absorption onsets/electronic origins of the emission observed for 3G1−1S (2.70 eV/2.65 eV) and 4G1−1S (2.53 eV/2.42 eV) are shifted to lower energy by 170/160 meV (3G1−2S) and 140/80 meV (4G1−2S) on incorporation of a bithiophene

(48) Gaab, K. M.; Thompson, A. L.; Xu, J. J.; Martinez, T. J.; Bardeen, C. J. *J. Am. Chem. Soc.* **2003**, *125*, 9288.

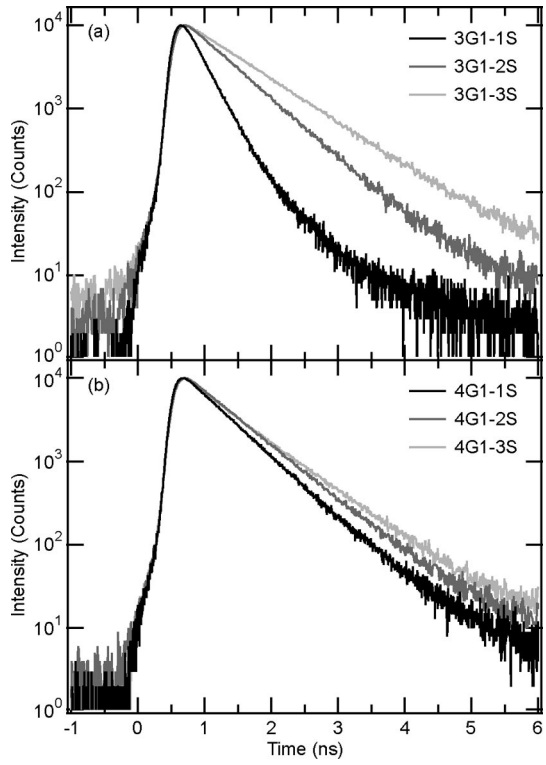

Figure 4. Fluorescence decay profiles, recorded after excitation at 438 nm, for the (a) 3-arm and (b) 4-arm dendrimers in degassed chloroform.

Table 2. Photoluminescence Properties of the First-Generation Phenyl-Cored Thiophene-Bridge Dendrimers in Degassed Chloroform

compd	E_{max}^{em} (eV (nm))[a]	ϕ_f (%)[b]	τ_f (ps)	τ_r (ns) τ_f/ϕ_f	SB^c	SB^d
3G1−1S	2.44 (508)	9 ± 1	250 ± 10	2.78 ± 0.33	2.16	3.61
3G1−2S (**7**)	2.31 (537)	23 ± 2	585 ± 20	2.54 ± 0.24	2.32	3.36
3G1−3S (**9**)	2.22 (558)	32 ± 3	800 ± 10	2.50 ± 0.24	2.12	3.02
4G1−1S	2.27 (546)	16 ± 2	560 ± 10	3.50 ± 0.44	2.14	3.89
4G1−2S (**11**)	2.32 (534)	21 ± 2	645 ± 15	3.07 ± 0.30	1.90	3.06
4G1−3S (**13**)	2.28 (544)	14 ± 2	675 ± 75[e]	4.82 ± 0.87	2.63	3.68

[a] Energy of emission maximum; wavelength in parentheses. [b] Quantum yields determined with respect to BASF Lumogen yellow 083 in degassed chloroform ($\phi \approx 95\%$). [c] Natural radiative lifetime, τ_r, calculated using the Strickler−Berg relationship with no limits for the integral of the modified absorption spectrum. [d] Natural radiative lifetime, τ_r, calculated using the Strickler−Berg relationship with an upper limit of 30 000 cm^{-1} for the integral of the modified absorption spectrum. [e] Fluorescence lifetime determined from the weighted average of biexponential fitting function.

bridging unit, with further shifts of 90/90 meV (3G1−3S) and 30/30 meV (4G1−3S) on the inclusion of a third thiophene ring. This trend is consistent with previous studies for series of para-poly(phenylene)s and oligothiophenes, where the increment of the spectral red-shift decreases with each added monomer unit.[43,49−51] The incremental red-shift is less than one would expect and is usually attributed to increasing thermal motion (rotation) of the thiophene rings, and therefore a diminishing coplanarity of the oligomers, with the extension of the length of the chain. The reduced red-shifts observed for the 4G1 series indicate that additional thiophene units produce a relatively smaller increase in the conjugation length, due to the already extensive conjugation along para-linked dendrimer arms.

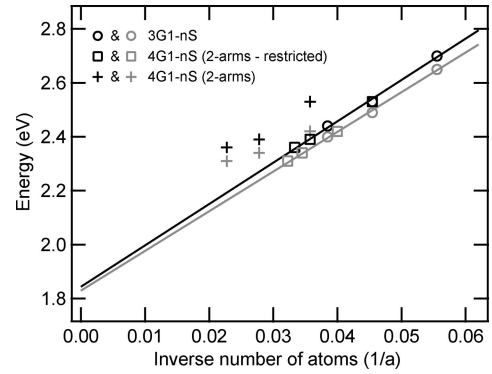

Figure 5. Absorption onset energy (black) and electronic origin of the emission (gray) versus the inverse number of atoms in the effective conjugation length of the chromophore. In the case of the 3-arm series, the effective conjugation length is assumed to be the α-conjugated segment plus the phenyl core (○), but for the 4-arm series the chromophore lengths are taken either as two complete α-conjugated segments plus the core (+) or two α-conjugated segments plus the core but shortened because of steric effects in the arms (□).

The dendrimers also show maxima at shorter wavelengths at approximately 320 and 250 nm, but the peak becomes less discernible with increasing thiophene bridge length. These shorter wavelength peaks have been previously attributed to excitations that are localized on shorter conjugated segments,[18] and indeed the absorption spectrum has been shown to consist of a superimposition of the absorption by multiple chromophores in the same wavelength region, corresponding to various conjugated subunits located within thiophene-based dendrons and dendrimers.[21] However, with increasing thiophene bridge length, the oscillator strength of the lowest excited-state along the α−α thiophene chain dominates the absorption, and the shorter wavelength peaks become less prominent.

The changes in the photoluminescence spectra, along with the observed trends in PL quantum yield and lifetime (Table 2), provide information about the relative spatial location of the "hot" and "cold" excitons and the interaction of the ground and excited states of the dendrimers with their environment. An extension of the dendron length results in a redistribution of the oscillator strength to the electronic origin (zero-phonon band) and an increase in the vibronic structure visible in the PL spectrum, similar to the trend observed for linear α-oligothiophenes.[50] These observations indicate that the electronic transition couples less strongly to both high (overall shape of vibronic progression) and low (width of vibronic bands) frequency vibrational modes, resulting in a reduced average Huang−Rhys parameter (Table 3) from the spectral fitting routine (see Experimental Section for full details). The implication is that there is a reduced geometrical rearrangement of the excited-state relative to the ground state (i.e., the "hot" and "cold" excitons are found at approximately the same location), resulting in the electronic transition coupling to fewer vibrational modes, although it should be noted that the role of dendrimer−solvent interactions cannot be ignored. In a previous theoretical study, comparison of the correlated electron−hole pair diagrams (CEHPD) for the 3G1 dendrimers confirms that

(49) Bauerle, P. *Adv. Mater.* **1992**, *4*, 102.
(50) Becker, R. S.; deMelo, J. S.; Macanita, A. L.; Elisei, F. *J. Phys. Chem.* **1996**, *100*, 18683.
(51) Martin, R. E.; Diederich, F. *Angew. Chem., Int. Ed.* **1999**, *38*, 1350.

Table 3. Results from Fitting a Franck−Condon Progression to the Photoluminescence Spectra

compd	E^{em}_{max} (eV (nm))[a]	$E^{em}_{0,0}$ (eV (nm))[b]	S[c]	ν_k (meV (cm^{-1}))[d]
3G1−1S	2.44 (508)	2.65 (468)	1.14	157.7 (1272)
3G1−2S (**7**)	2.31 (537)	2.49 (498)	1.17	169.1 (1364)
3G1−3S (**9**)	2.22 (558)	2.40 (517)	1.00	167.4 (1350)
4G1−1S	2.27 (546)	2.42 (512)	0.97	164.8 (1329)
4G1−2S (**11**)	2.32 (534)	2.34 (530)	0.90	172.0 (1387)
4G1−3S (**13**)	2.28 (544)	2.31 (537)	0.89	171.4 (1382)

[a] Energy of emission maximum; wavelength in parentheses. [b] Electronic origin of emission (defined as the energy of the transition between the lowest vibrational levels of the excited-state and ground state); wavelength in parentheses. [c] Huang−Rhys parameter (see Experimental Section for full details). [d] Average energy of vibrational modes that couple to the electronic transition (see Experimental Section for full details).

the spatial extent of the "hot" and "cold" excitons are increasingly similar as the thiophene bridge length increases,[4] consistent with the spectral observations presented here. The reduced electron−phonon coupling is also manifested in an increase of the fluorescence quantum yield and lifetime with increasing dendron length; the trend observed for the 3-arm dendrimers is consistent with the increase measured for linear α-oligothiophenes.[50] The apparent deviation of the 4G1−3S sample from the trend may be attributed to the biexponential function required to satisfactorily describe the fluorescence decay curve, because of the increased degrees of freedom of the larger molecule. A similar feature was also observed for another related dendrimer, 4G2−1S,[20] reported previously. The reason behind this phenomenon is currently being investigated further.

The experimentally determined natural radiative lifetime, τ_r (given by τ_f/ϕ_f), is ca. 2.6 ns across the 3G1 series, suggesting that the nature of the "cold" exciton is similar for the 3-arm dendrimers; this value is almost identical to those calculated from the photoluminescence data obtained for a series of linear α-oligothiophenes.[50] This is not the case for the 4G1 dendrimers, where no obvious trend is observed, implying that the nature of the emitting exciton is noticeably different as the length of the thiophene bridge increases. As mentioned earlier, this is consistent with the extent of structural reorganization predicted by ab initio methods for the 4-arm dendrimers after excitation,[4] which decreases with dendron length, and is also consistent with the observed reduction in the Huang−Rhys factor (Table 3).

The difference between the values predicted for the 3- and 4-arm dendrimers suggest that the nature of the emitting chromophore is different between the two series (and particularly for 4G1−3S), even though the dendrimers are quite similar in structure, consistent with theoretical calculations predicting significant differences between the spatial location of the "hot" and "cold" excitons in the 3G1 and 4G1 series.[4] In contrast, Strickler−Berg (SB) analysis[52,53] (see Experimental Section for full details) of the modified absorption and emission spectra predict natural radiative lifetimes of 2.21 ± 0.25 ns for all the dendrimers, implying that the nature of the emitting species is similar. Although the τ_r values predicted by SB analysis are shorter than the experimentally determined values (Table 2), it should be noted that this calculation involved full integration of the absorption spectrum and as such includes contributions from higher-lying excited states. The presence of these higher-energy states is predicted by comparison of the mirror image of the modified emission spectrum with the modified absorption spectrum (see Figure S1 in the Supporting Information).[52,53] Integration of the lowest energy absorption band, to an upper energy limit of 30 000 cm^{-1}, to reduce the contribution from these higher energy excited states, increases the calculated τ_r values to 3.44 ± 0.35 ns (Table 2). Although this is more consistent with the values determined from the fluorescence quantum yields and lifetimes for 4G1−1S and 4G1−2S, it is still a significant underestimate of τ_r for 4G1−3S.

Conclusions

The 3G1-*n*S and 4G1-*n*S series of dendrimers were successfully synthesized, purified and characterized for n = 1,[20] 2, and 3. These molecules enable the effects of coupling of the oligothiophene dendrons to, and through, the phenyl core to be investigated. The electronic and optical properties demonstrate that for the 3G1 series, the chromophore corresponds to the phenyl core coupled to all the thiophene units that are alpha-linked in the arm, with the electronic and optical bandgaps decreasing with increasing number of bridging thiophene units, n. For the 4G1 series, the chromophore couples through the phenyl core, connecting predominantly the para-linked arms. Here, like the conjugated polymer analogue poly(3-hexylthiophene), the chromophore resides over a sequence that is less than the full possible length of conjugation, although both the electronic and optical bandgaps still increase with n.

The emission properties of the 3G1 series therefore exhibit properties that are strongly linked to the length of the dendrons, showing an increase in PL lifetime and quantum yield. For the 4G1 series, the same is not true, with the emission, and hence the nature of the relaxed (or cold) exciton, being very similar in all three cases, with PL lifetimes and quantum yields that appear independent of n. In contrast, the natural radiative lifetimes of the 3-arm dendrimers are quite constant, whereas for the 4-arm dendrimers they vary and are actually longer than the 3G1 series. This is inconsistent with the larger extinction coefficient for the 4-arm dendrimers, which would predict a shorter natural radiative lifetime. The difference reveals a significant change between the nature of the initial, "hot" exciton formed upon photon absorption, and the final, "cold" emissive exciton for the 4G1 series, a difference that is not seen for the 3G1 series. It appears that the chromophores within the 3-arm dendrimers behave like molecular entities, i.e., the absorbing and emitting species are geometrically similar, whereas for the 4-arm dendrimers, the "hot" and "cold" excitons are geometrically different, due to structural relaxation permitted by the increased size of the chromophore. As a result, the 4-arm dendrimers begin to show photophysical properties (i.e., significant downhill energy relaxation) similar to their polymer analogues.

(52) Strickler, S. J.; Berg, R. A. *J. Chem. Phys.* **1962**, *37*, 814.
(53) Birks, J. B. *Photophysics of Aromatic Molecules*; John Wiley & Sons: London, 1970.

These and other studies of dendrimers provide a useful foundation for understanding the photophysics of conjugated polymers with similar conjugation sequences. Further studies of thin films, to include optical properties, X-ray diffraction, charge carrier mobilities, and OPV device data will demonstrate whether these classes of molecules can usurp their polymer counterparts as active components in excitonic solar cells.

Experimental Section

General Procedures. ^{1}H and ^{13}C NMR spectra were recorded on a Varian unity INOVA AS400 spectrometer: chemical shifts are reported in parts per million (ppm) relative to residual solvent. Elemental analysis was performed by Huffman Laboratories, Golden, CO. All electronic absorption spectra were taken as solutions in DCM using a Hewlett-Packard 8453 spectrophotometer. Absorption onset energies were taken as the low energy onset to absorption and were calculated as the intersection of two tangents, one along the baseline and the other at the point of inflection on the low-energy edge of the initial absorption. Emission spectra were recorded on a Jobin-Yvon Fluorolog 3 fluorescence spectrometer with a cooled CCD detector. All spectra were corrected for the response of the detection system. Fluorescence quantum yields were determined relative to a perylene dye (BASF Lumogen yellow 083) in degassed chloroform, which has a quantum yield close to 100%. Fluorescence decays were recorded using time-correlated single-photon counting, with pulsed diode laser excitation at 438 nm (Jobin Yvon IBH). Emission was monitored perpendicular to excitation through a 0.25 m monochromator and detected using a cooled photon counting photomultiplier tube (Hamamatsu H6279), which gave a response function of 225 ps. Data were analyzed using a nonlinear least-squares iterative reconvolution routine using established procedures.[54] The finite width of the instrument response function was effectively deconvoluted from the measured data to give an overall temporal response of ca. 20 ps. Data were fit to a sum of either one or two exponentials, and the quality of fit was judged using stringent statistical procedures.[54]

Strickler−Berg Analysis. The natural radiative rate constant (k_r), which is defined as the reciprocal of the natural radiative lifetime (τ_r), can be calculated from the integral of the modified absorption spectrum and is given by[52,53]

$$k_r = 1/\tau_r = 2.88 \times 10^{-9} \frac{n_f^3}{n_a} \langle \bar{\nu}_f^{-3} \rangle_{avg}^{-1} \int_{\bar{\nu}=0\ cm^{-1}}^{\infty} \frac{\varepsilon(\nu)}{\nu}\, d\nu \quad (1)$$

where n_f and n_a are the refractive indices of the solvents in which the fluorescence and absorption spectra are measured, respectively, $\varepsilon(\nu)/\nu$ is the modified absorption spectrum and $\langle \bar{\nu}_{f-3)_{avg}} \rangle$ is the reciprocal of the mean value of ν^{-3} over the fluorescence spectrum, which is equivalent to

$$\langle \bar{\nu}_f^{-3} \rangle_{avg}^{-1} = \frac{\int F(\nu)\, d\nu}{\int \frac{F(\nu)\, d\nu}{\nu^3}} \quad (2)$$

When the mirror image of the modified emission spectrum does not describe the absorption spectrum accurately, as is the case for all the dendrimers studied here (see Figure S1 in the Supporting Information), errors are introduced into the calculated natural radiative lifetime and it becomes necessary to minimize the contribution of higher energy excited states to the integrated area of the modified absorption spectrum.[52,53] To this end, τ_r was also calculated using an upper energy limit of 30 000 cm^{-1} for the integral in eq 1 (see Table 2):

$$\int_{\bar{\nu}=0\ cm^{-1}}^{30\,000\ cm^{-1}} \frac{\varepsilon(\nu)}{\nu}\, d\nu \quad (3)$$

Spectral Fitting Routine. The emission spectra of the dendrimers were modeled following a method similar to that employed to calculate the optical spectra of oligophenylenevinylenes.[55] This approach assumes an approximation of displaced, but undistorted, harmonic oscillators (i.e., the vibrational frequency of the ground and excited states is identical). Within this approximation the electron−phonon coupling constant, or Huang−Rhys parameter (S),[56] is related to the projected geometry change between the ground and excited states, ΔQ_k

$$S = \frac{2\pi^2 c}{h} v_k (\Delta Q_k)^2 \quad (4)$$

where c is the velocity of light, h is Planck's constant, and ν_k is the considered vibrational mode. Because many vibrational modes couple to the electronic transition, the value of ν_k obtained from the spectral fit is an average, although it often corresponds to the frequency of a dominant vibrational mode. The Franck−Condon (FC) factors, $F_{0,k}$, which are a measure of the overlap between the wave functions of the zeroth vibrational level of the initial (excited) state and the kth vibrational level of the final (ground) state, are then calculated using

$$F_{0,k} = \frac{S^k e^{-S}}{k!} \quad (5)$$

The individual spectral lines are subsequently broadened by a normalized Voigt function, $I_V(\nu)$, which is calculated using an algorithm formalized by Humlicek[57] and discussed in greater detail by Schreier.[58] The Voigt function is chosen because the optical transitions of organic chromophores can be homogeneously and inhomogeneously broadened, resulting in the peak profile being a convolution of Lorentzian, $I_L(\nu)$, and Gaussian, $I_G(\nu)$, lineshapes. The final modeled spectrum, $I(\nu)$, is given by the sum of the individual Voigt peaks representing the vibronic progression, such that the amplitude of vibronic peak k is $A_{tot}F_{0,k}$

$$I(\upsilon) = \sum_{k=0}^{p} A_{tot} F_{0,k} I_V(\upsilon) = \sum_{k=0}^{p} A_{tot} F_{0,k} [I_G(\upsilon) \otimes I_L(\upsilon)] \quad (6)$$

The line shape of the Voigt function is governed by parameters affecting the position ($E_{0,k}^{em} = E_{0,0}^{em} - k\upsilon_k$, where $E_{0,0}^{em}$ is the electronic origin), width (γ_V), and shape (σ_V), a weighting factor that determines the contribution from the Gaussian and Lorentzian components. Nonlinear, least-squares optimization (Levenberg−Marquardt algorithm) is used to minimize chi-square,[59] by comparison of the modeled and measured spectra.

Synthesis. All chemicals were purchased from Sigma-Aldrich and were used as received without further purification. Tetrahy-

(54) Phillips, D.; O'Connor, D. V. *Time-Correlated Single-Photon Counting*; Academic Press: London, 1984.
(55) Gierschner, J.; Mack, H. G.; Luer, L.; Oelkrug, D. *J. Chem. Phys.* **2002**, *116*, 8596.
(56) Huang, K.; Rhys, A. *Proc. R. Soc. London, Ser. A* **1950**, *204*, 406.
(57) Humlicek, J. *J. Quant. Spectrosc. Radiat. Transfer* **1982**, *27*, 437.
(58) Schreier, F. *J. Quant. Spectrosc. Radiat. Transfer* **1992**, *48*, 743.
(59) Press, W. H.; Flannery, B. P.; Teukolsky, S. A.; Vetterling, W. T. *Numerical Recipes in C*, 2nd ed.; Cambridge University Press: New York, 1992.

drofuran was dried over sodium and freshly distilled prior to use. All reactions were performed under argon, using glassware that was flame dried and then cooled under a stream of argon. Starting materials and intermediates were prepared according to literature methods: 5,5″-dihexyl-[2,2′;3′,2″]terthiophene (**1**),[24] tributyl-(5,5″-dihexyl-[2,2′;3′,2″]terthiophen-5′-yl)stannane (**2**),[24] 2-bromo-5-(thiophen-2-yl)thiophene (**3**),[60] 1,3,5-tri(2′-bromo-5′-thienyl)benzene (**8**),[20] and 1,2,4,5-tetra(2′-bromo-5′-thienyl)benzene (**12**).[20]

*5,5′′′′-Dihexyl-[2,2′;5′,2″;5″,2‴;3′,2′′′′]pentathiophene (**4**).* A mixture of tributyl-(5,5″-dihexyl-[2,2′;3′,2″]terthiophen-5′-yl)stannane **2** (14.8 g, 21 mmol), 2-bromo-5-(thiophen-2-yl)thiophene **3** (4.1 g, 17 mmol), and dry *N*,*N*-dimethylformamide (60 cm^3) was degassed with argon for 10 min. Tetrakis(triphenylphosphine) palladium (0) (400 mg, 0.35 mmol) was then added and the mixture heated at 90 °C for 17 h. After allowing it to cool, the solvent was removed in vacuo. Ether (300 cm^3) was added and the organic washed with aqueous potassium fluoride solution (2 × 50 cm^3) with filtration between washings. The organic was then washed with water (100 cm^3) before being dried over anhydrous magnesium sulfate. Filtration and removal of the solvent in vacuo then followed. The crude product was then purified by column chromatography (ethyl acetate:hexanes, 1:99) to give **4** (8.0 g, 82%) as a yellow oil, which solidified at low temperatures. Found: C, 66.41; H, 6.35 $C_{32}H_{36}S_5$. Requires: C, 66.16; H, 6.25%. λ_{max} (CH_2Cl_2) (nm) 252 (log ε (dm^3 mol^{-1} cm^{-1}) 4.29), 330 (4.21) and 390 (4.42). δ_H (400 MHz; $CDCl_3$) 0.87−0.93 (6 H, m), 1.26−1.41 (12 H, m), 1.65 (2 H, qu, *J* 8.0), 1.67 (2 H, qu, *J* 8.0), 2.77 (2 H, t, *J* 8.0), 2.79 (2 H, t, *J* 8.0), 6.66−6.69 (2 H, m), 6.90 (1 H, d, *J* 3.6), 6.96 (1 H, d, *J* 3.6), 7.01 (1 H, dd, *J* 3.6, 5.2), 7.06 (1 H, d, *J* 3.6), 7.07 (1 H, d, *J* 3.6), 7.16 (1 H, s), 7.17 (1 H, dd, *J* 1.6, 3.6) and 7.21 (1 H, dd, *J* 1.6, 5.2). δ (100 MHz; $CDCl_3$) 14.4, 22.9, 29.0, 30.4, 31.8, 31.9, 124.0, 124.4, 124.5, 124.6, 124.7, 124.8, 126.4, 126.7, 127.7, 128.2, 130.9, 132.3, 132.6, 134.6, 135.0, 135.7, 136.7, 137.3, 146.6 and 147.9. *m*/*z* (MALDI-TOF-ES+) 580.26 (100%) [M^+] (calcd, 580.14).

*1,3,5-Tri(5′′′′,5′′′′′-dihexyl-[2′,5″;2″,5‴;2‴,2′′′′;3′′′,2′′′′′]pentathiophen-5′-yl)benzene [3G1−2S] (**7**).* To a solution of G1−2S dendron **4** (465 mg, 0.80 mmol) in dry tetrahydrofuran (4 cm^3) was added *n*-butyllithium (2.5 M in hexanes, 0.36 cm^3, 0.90 mmol) dropwise at −78 °C. After addition, the reaction mixture was stirred at −78 °C for 15 min before removal of the ice-bath and stirring for a further 1 h. Tributyltin chloride (0.24 cm^3, 0.90 mmol) was then added dropwise followed by stirring at room temperature for 2 h. Water (100 cm^3) was added and the product extracted with ether (2 × 100 cm^3). The organic extracts were combined, dried over anhydrous magnesium sulfate, filtered and the solvent removed in vacuo to give **5** as a yellow-orange oil. The crude product was used without further purification. δ_H(400 MHz; $CDCl_3$) 0.82−0.93 (15 H, m), 1.07−1.14 (6 H, m), 1.23−1.40 (18 H, m), 1.52−1.68 (10 H, m), 2.75 (2 H, t, *J* 7.2), 2.77 (2 H, t, *J* 7.2), 6.65−6.67 (2 H, m), 6.88 (1 H, d, *J* 3.6), 6.93 (1 H, d, *J* 3.6), 7.04−7.08 (3 H, m), 7.14 (1 H, s) and 7.28 (1 H, d, *J* 3.6). A mixture of crude stannane **5**, 1,3,5-tribromobenzene **6** (63 mg, 0.2 mmol), and dry *N*,*N*-dimethylformamide (1.5 cm^3) was degassed with argon for 10 min. Tetrakis(triphenylphosphine) palladium (0) (20 mg, 0.02 mmol) was then added and the mixture heated at 90 °C for 50 h. After being allowed to cool, acetone (10 cm^3) was added and the mixture filtered, followed by washing of the solid with acetone until the filtrate was colorless. The residue was then dried under a vacuum to give **7** (310 mg, 85%) as a brown solid, mp 101 °C. Found: C, 67.06; H, 6.02. $C_{102}H_{108}S_{15}$ requires: C, 67.50; H, 6.00%. λ_{max} (CH_2Cl_2)/nm 252 (logϵ/$dm^3mol^{-1}cm^{-1}$ 4.53) and 423 (4.81). δ_H (400 MHz; $CDCl_3$) 0.88 (18 H, t, *J* 6.4), 1.23−1.40 (36 H, m), 1.64 (6 H, qu, *J* 8.0), 1.66 (6 H, qu, *J* 8.0), 2.76 (6 H, t, *J* 8.0), 2.78 (6 H, t, *J* 8.0), 6.64−6.68 (6 H, m), 6.89 (3 H, d, *J* 3.6), 6.94 (3 H, d, *J* 3.6), 7.07 (3 H, d, *J* 4.0), 7.11 (3 H, d, *J* 4.0), 7.15 (3 H, d, *J* 3.6), 7.16 (3 H, s), 7.31 (3 H, d, *J* 3.6) and 7.65 (3 H, s). δ_C (100 MHz; $CDCl_3$) 14.3, 22.8, 29.0, 30.4, 31.7, 31.8, 121.6, 124.3, 124.4, 124.6, 124.7, 126.3, 126.7, 127.6, 130.9, 132.3, 132.5, 134.6, 134.9, 135.4, 135.9, 136.4, 137.2, 142.2, 146.6 and 147.8. *m*/*z* (MALDI-TOF-ES+) 1814.04 [MH^+] (calcd, 1812.43).

*1,3,5-Tri(5′′′′,5′′′′′-dihexyl-[2′,5″;2″,5‴;2‴,5′′′′;2′′′′,2′′′′′;3′′′′, 2′′′′′]sexithiophen-5′-yl)benzene [3G1−3S] (**9**).* The 3G1−3S dendrimer **9** was prepared in a similar manner to **7** using a mixture of crude stannane **5**, prepared as described above, 1,3,5-tri(2′-bromo-5′-thienyl)benzene **8** (110 mg, 0.2 mmol), dry *N*,*N*-dimethylformamide (1.5 cm^3), and tetrakis(triphenylphosphine) palladium (0) (20 mg, 0.02 mmol) to give **9** (360 mg, 88%) as a dark red solid, mp 129 °C. Found: C, 66.05; H, 5.58. $C_{114}H_{114}S_{18}$ requires: C, 66.43; H, 5.57%. λ_{max} (CH_2Cl_2)/nm 256 (logϵ/$dm^3mol^{-1}cm^{-1}$ 4.76) and 440 (5.12). δ_H (400 MHz; $CDCl_3$) 0.81−0.91 (18 H, m), 1.19−1.39 (36 H, m), 1.59−1.70 (12 H, m), 2.75 (6 H, t, *J* 8.0), 2.77 (6 H, t, *J* 8.0), 6.64−6.68 (6 H, m), 6.88 (3 H, d, *J* 3.6), 6.93 (3 H, d, *J* 3.6), 7.06 (3 H, s), 7.08 (3 H, d, *J* 3.6), 7.12 (3 H, d, *J* 3.6), 7.14 − 7.18 (9 H, m), 7.32 (3 H, d, *J* 3.6) and 7.65 (3 H, s). *m*/*z* (MALDI-TOF-ES+) 2059.90 [MH^+] (Calcd. 2058.39).

*1,2,4,5-Tetra(5′′′′,5′′′′′-dihexyl-[2′,5″;2″,5‴;2‴,2′′′′;3‴,2′′′′′]pentathiophen-5′-yl)benzene [4G1−2S] (**11**).* Stannane **5** was prepared, as described above in the preparation of **7**, from **4** (991 mg, 1.7 mmol) and *n*-butyllithium (2.5 M, 0.78 cm^3, 1.9 mmol) in 6 mL of THF followed by tributyltin chloride (0.51 cm^3, 1.9 mmol). Crude **5** was combined with 1,2,4,5-tetrabromobenzene **10** (125 mg, 0.32 mmol), dry *N*,*N*-dimethylformamide (3 cm^3), and tetrakis(triphenylphosphine) palladium (0) (30 mg, 0.03 mmol) and heated under an inert atmosphere, as described in the preparation of **7**, to give **11** (720 mg, 94%) as an orange/red solid, mp 136 °C. Found: C, 67.01; H, 6.16. $C_{134}H_{142}S_{20}$ requires: C, 67.23; H, 5.98%. UV λ_{max} (CH_2Cl_2) (nm) 250sh (log ε (dm^3 mol^{-1} cm^{-1}) 5.01), 301 (4.94) and 422 (5.19). δ_H (400 MHz; $CDCl_3$) 0.88 (24 H, t, *J* 7.0), 1.23−1.40 (48 H, m), 1.64 (8 H, qu, *J* 7.0), 1.65 (8 H, qu, *J* 7.0), 2.75 (8 H, t, *J* 7.0), 2.77 (8 H, t, *J* 7.0), 6.63−6.68 (8 H, m), 6.88 (4 H, d, *J* 3.6), 6.91 (4 H, d, *J* 4.0), 6.93 (4 H, d, *J* 3.6), 7.02−7.09 (12 H, m), 7.14 (4 H, s) and 7.66 (2 H, s). δ_C (100 MHz; $CDCl_3$) 14.3, 22.8, 29.0, 30.4, 31.7, 31.8, 124.2, 124.3, 124.5, 124.7, 126.4, 126.7, 127.6, 128.8, 130.9, 132.3, 132.6, 132.9, 134.6, 134.9, 135.9, 136.4, 138.3, 140.4, 146.6 and 147.9. *m*/*z* (MALDI-TOF-ES+) 2391.80 [MH^+] (calcd, 2390.55).

*1,2,4,5-Tetra(5′′′′,5′′′′′-dihexyl-[2′,5″;2″,5‴;2‴,5′′′′;2′′′′,2′′′′′;3′′′′, 2′′′′′]sexithiophen-5′-yl)benzene [4G1−3S] (**13**).* The 4G1−3S dendrimer **13** was prepared in a manner similar to that of **7** using a mixture of crude stannane **5**, as described for the preparation of **7**, 1,2,4,5-Tetra(2′-bromo-5′-thienyl)benzene **12** (116 mg, 0.16 mmol), dry *N*,*N*-dimethylformamide (1.5 cm^3) and tetrakis(triphenylphosphine) palladium (0) (20 mg, 0.02 mmol). The product was also purified similar to **7** to give **13** (370 mg, 86%) as a red solid, mp 160 °C. Found: C, 65.87; H, 5.93. $C_{150}H_{150}S_{24}$ requires: C, 66.18; H, 5.55%. UV λ_{max} (CH_2Cl_2) (nm) 255 (log ε (dm^3 mol^{-1} cm^{-1}) 4.83), 304 (4.60) and 442 (5.15). δ_H (400 MHz; $CDCl_3$) 0.87 (24 H, t, *J* 7.0), 1.23−1.39 (48 H, m), 1.63 (8 H, qu, *J* 7.0), 1.65 (8 H, qu, *J* 7.0), 2.75 (8 H, t, *J* 7.0), 2.77 (8 H, t, *J* 7.0), 6.64−6.67 (8 H, m), 6.88 (4 H, d, *J* 3.6), 6.91 (4 H, d, *J* 3.6), 6.93 (4 H, d, *J* 3.6), 7.03−7.09 (20 H, m), 7.14 (4 H, s) and 7.66 (2 H, s). δ_C (100 MHz; $CDCl_3$) 14.3, 22.8, 29.0, 30.4, 31.7, 31.8, 124.2, 124.3, 124.4, 124.6, 124.7, 126.4, 126.7, 127.6, 128.8, 130.9, 132.3, 132.5, 132.8, 133.5, 134.6, 134.9, 135.8, 136.2, 136.3, 138.3, 140.4, 146.6 and 147.8. *m*/*z* (MALDI-TOF-ES+) 2720.40 [MH^+] (calcd, 2718.50).

(60) Bauerle, P.; Wurthner, F.; Gotz, G.; Effenberger, F. *Synthesis* **1993**, 1099.

Acknowledgment. The authors thank Bill McMahon for help in the MALDI-TOF-MS measurements. Support of this work by the NREL LDRD program and the Xcel Energy Renewable Development Fund is gratefully acknowledged. A.J.F. and G.R. were funded by the Photochemistry and Radiation Research program of the U.S. Department of Energy, Office of Science, Basic Energy Sciences, Division of Chemical Sciences, Geosciences and Biosciences, under Contract DEAC36−99GO10337 to NREL.

Supporting Information Available: Discussion of the mass properties, thermal decomposition, and electronic properties, including a comparison of the electronic and optical band gaps of the dendrimers; figures include MALDI-TOF mass spectra, typical TGA traces, and cyclic voltammograms (PDF). This material is available free of charge via the Internet at http://pubs.acs.org.

CM802410D